Analytica Chimica Acta 686 (2011) 144–149

Contents lists available at ScienceDirect

Analytica Chimica Acta

journal homepage: www.elsevier.com/locate/aca

An enzyme-free quartz crystal microbalance biosensor for sensitive glucose detection in biological fluids based on glucose/dextran displacement approach

Dianping Tang[a,b,*], Qunfang Li[a,b], Juan Tang[a,b], Biling Su[a,b], Guonan Chen[a,b,*]

[a] Ministry of Education Key Laboratory of Analysis and Detection for Food Safety, Department of Chemistry, Fuzhou University, Fuzhou 350108, PR China
[b] Fujian Provincial Key Laboratory of Analysis and Detection Technology for Food Safety, Department of Chemistry, Fuzhou University, Fuzhou 350108, PR China

ARTICLE INFO

Article history:
Received 22 October 2010
Received in revised form
28 November 2010
Accepted 30 November 2010
Available online 8 December 2010

Keywords:
Displacement approach
Graphene nanosheets
Glucose
Nonenzyme biosensor
Quartz crystal microbalance

ABSTRACT

A sensitive and facile quartz crystal microbalance (QCM) biosensor for glucose detection in biological fluids was developed by means of a displacement-type assay mode between glucose and its analogy dextran for concanavalin A (ConA) binding sites on a graphene-based sensing platform. To construct such a displacement-based sensor, phenoxy-derived dextran (DexP) molecules were initially assembled onto the surface of graphene-coated QCM probe *via* π–π stacking interaction, and ConA molecules were then immobilized on the dextran through the dextran-ConA interaction. Upon addition of glucose, the analyte competed with the dextran for the ConA, and displaced it from the QCM probe, leading to a change in the frequency. Under optimal conditions, the frequency change relative to the basic resonant frequency was proportional to glucose concentration, and exhibited a dynamic range from 0.01 to 7.5 mM with a low detection limit (LOD) of 5.0 μM glucose (at 3σ). The relative standard deviations (RSDs) were below 6.2% and 9.0% for the reproducibility and selectivity of the QCM glucose sensors, respectively. In addition, the assay system was evaluated with glucose spiking samples into the distilled water and blank cattle serum, receiving in excellent correlation with the referenced values.

1. Introduction

Glucose, a primary source of energy in our body, is an important carbohydrate in biology. Based on the clinical practical recommendations, it circulates in the blood at a normal concentration of 3.3–6.1 mM [1]. High levels of glucose most frequently indicate diabetes, but many other diseases and conditions might also elevate glucose concentrations [2]. The opposite, extremely low glucose levels, can result from too little food or variable insulin excretion [3]. Thus, frequent testing of physiological glucose levels is critical to confirm that treatment is working effectively, and to avoid a diabetic emergency, such as hypoglycemia (low blood sugar: <3 mM) or hyperglycemia (high blood sugar: >7 mM) [4].

Recently, various sensing techniques including noninvasive glucose sensors and enzyme-based biosensors have been developed for detection of glucose [5–9]. As noninvasive glucose sensors could usually avoid the direct contact between the transducer and the representative biological fluid, the challenge is to make an accurate measurement without the aid of selective chemical reagents or physical separations [10]. Up to date there is no resulting product on the market, however. For the commercially available glucose enzyme biosensors, several drawbacks are often puzzled in long-term clinical practice, such as impaired responses and unpredictable drift in the *in vivo* signal, which necessitate frequent calibration against finger-prick samples [11,12]. Meanwhile, the enzyme-based glucose biosensors display the insufficient long-term stability due to the bioactivity of the immobilized enzymes [13]. So, searching for a nonenzyme-based sensor for glucose detection with substantial improvement in sensitivity and selectivity is of considerable interest.

Generally, the measurement principle of the nonenzyme-based biosensors is based on glucose electro-oxidation using nanocatalysts or the displacement-based assay mode using an analyte analogy [14–18]. A main drawback for nanocatalyst-based glucose sensors is that various endogenous interfering species including uric acid, ascorbic acid and 4-acetamidophenol might be oxidized in the potential range of glucose oxidation, thus resulting in a poor selectivity. In this regard, the displacement-based assay mode similar to the competitive-type immunoassay format could overcome the shortcoming to some extent [19]. Concanavalin A (Con A), a lectin protein with four saccharide bind sites extracted from the *jack-bean*, binds specifically to certain structures found in various sugars, glycoproteins and glycolipids, mainly internal and nonreducing terminal alpha-mannosyl groups [20]. Since the affinity of ConA molecule for the mannose and glucose is well known, the

* Corresponding authors at: Ministry of Education Key Laboratory of Analysis and Detection for Food Safety, Department of Chemistry, Fuzhou University, Fuzhou 350108, PR China. Tel.: +86 591 2286 6125; fax: +86 591 2286 6135.
E-mail addresses: dianping.tang@fzu.edu.cn, dianping.tang@hotmail.com (D. Tang), gnchen@fzu.edu.cn (G. Chen).

0003-2670/$ – see front matter © 2010 Elsevier B.V. All rights reserved.
doi:10.1016/j.aca.2010.11.054

glucose-ConA-dextran systems are often employed for detection of glucose [21,22]. Related to transducers, quartz crystal microbalance (QCM) has become an analytical tool for investigations of biomolecular interactions and clinical bioassays due to high sensitivity, low cost, real time output, and label- or radiation-free entities [23,24]. The QCM sensors measure the resonant frequency (f) using the standard oscillator technique. The frequency shift (Δf) is usually explained by Sauerbrey equation, which states that the frequency shift is linearly proportional to the change of surface mass (Δm) on the crystal [25]. Sauerbrey equation, however, holds only for the case of rigid coated material [26]. The qualitative aspects of the resulting data and the magnitude of the observed effect are shown to be independent of film thickness for values as low as 115 Å [23–26]. When an overlayer is thick, the relationship between the Δf and Δm is no longer linear and corrections are necessary.

Coupling nanomaterials with biomolecular recognition events have proven of particular utility in this regard due to their unique optical, electronic, and catalytic properties [27,28]. Great attention has been drawn toward the design of nanomaterials-based biosensors based on the interactions between biomolecules and nanomaterials of different compostions, dimensions and shapes [29]. Graphene, a one-atom thick and two-dimensional sheet of carbon atoms arranged in a honeycomb-like structure, has extensively used as sensing elements because of its excellent electrical properties, ultrahigh ratio of surface area to volume, and the extreme sensitivity of its surface atoms to any surface adsorption/reaction events [30,31]. In this study, we employed graphene nanosheets as an affinity support for the immobilization of biomolecules on the QCM crystal. The displacement-based QCM assay systems are generally operated by taking advantages of the competitive binding between a target analyte and analogue for a protein-binding site. Glucose as a small molecule (MW 180.2) might be ineffective based on direct detection by using the traditional modes of affinity-based sensing, since their binding to the recognition molecules might not generate an obviously measurable change in the frequency. Signal amplification is necessary.

Herein we designed an amplified QCM assay protocol for sensitive detection of glucose by using ConA molecules as traces with a displacement-based mode on the ConA/phenoxydextran/graphene-based QCM probe. The dextran, as an analogue of glucose, has a lower affinity for binding to ConA molecule than that of glucose. Upon addition of glucose into the detection cell, it competes with the dextran for ConA binding sites and displaces it from the QCM probe, leading to a change in the frequency. As the molecular weight (MW) of ConA is far more than that of glucose, we anticipate that the displaced ConA molecules could generate a signalling amplification of QCM response. The aim of this study is to design an enzyme-free QCM sensing platform for sensitive detection of glucose in biological fluids based on glucose/dextran displacement approach.

2. Experimental

2.1. Chemicals

Concanavalin A (ConA) from *Canavalia ensiformis* (Jack bean) (Type VI, lyophilized power, MW 26.5 kDa), D-glucose ($C_6H_{12}O_6{\cdot}H_2O$), 1,2-epoxy-3-phenoxypropane and dextran were purchased from Sigma–Aldrich (USA). D-Ascorbic acid (AA, $C_6H_8O_6$, 99% purity), uric acid (UA, 99% purity), bovine serum albumin (BSA) and 4-acetamidophenol (AP) were obtained from Beijing Chem. Re. Ltd. Co. (Beijing, China). Graphene (GP) was gifted from Yang Lab of our group, and the synthesized process and characteristics of graphene were described in the recently published paper [32]. All gold-coated quartz crystals were purchased from Shanghai CHI Instrument Co. (Shanghai, China). Blank cattle serum samples were purchased from Dingguo Biotechnology Ltd. Co. (Beijing, China). All other reagents were of analytical grade.

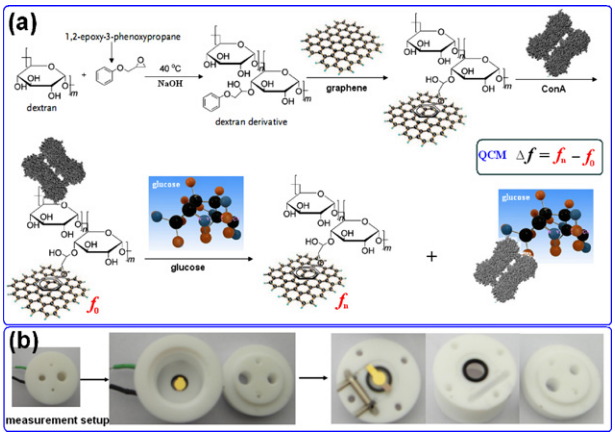

Scheme 1. (a) Fabrication process and measurement principle of the displacement-based QCM glucose sensor and (b) the QCM measurement setup.

2.2. Synthesis of 1,2-epoxy-3-phenoxypropane-derivated dextran (DexP)

1,2-Epoxy-3-phenoxypropane-derivated dextran (DexP) was synthesized similar to previously published method [33] as illustrated in Scheme 1a. It consists of a two-step reaction as follows: (i) dextran molecules were allowed to react with 1,2-epoxy-3-phenoxypropane in the presence of $Zn(BF_4)_2$, and (ii) the resulting derivative was treated with an aqueous solution of phenol at pH 11 and at room temperature (RT) for 24 h. The crude product was precipitated twice with ethanol and treated with 1 M NaOH for 48 h to remove all the unreacted chemicals. Finally, the obtained hydrophobic dextran derivatives (DexPs) were dialyzed against water and freeze-dried.

2.3. Preparation of QCM sensors

Prior to the bottom-up layer formation process, quartz crystals coated with a gold film were extensively cleaned according to our previously reported protocol [34]. Following that, the QCM probe was blow-dried under N_2 and placed into the measurement chamber. Distilled water was added into the chamber to reach a steady state. Afterwards, 500 μL of graphene nanosheets (5.0 mg mL^{-1}) was injected into the chamber, and incubated for ~20 min at RT, in order to make graphene nanosheets adsorb on the surface of gold substrate. After the detection cell was washed with distilled water, 500 μL of DexP solution (3.0 μM) was further injected into the cell, and the DexP molecules were adsorbed on the surface of graphene due to π–π stacking interaction between graphene and DexPs. Subsequently, 500 μL of ConA solution (15 μM) was added into the chamber. In the presence of dextran, the ConA molecules were conjugated on the DexP. The as-prepared QCM probe (designed as ConA/DexP/GP/Au) was stored at 4 °C when not in use.

2.4. Measurement process

QCM measurements were performed out on CHI 430a electrochemical quartz crystal microbalance system (Shanghai, China) controlled by a laptop under Windows environment. The QCM system contained an external box with oscillator circuitry and a QCM detection cell. The cell consisted of three round Teflon pieces. The top piece was the cell top to hold reference and counter electrodes,

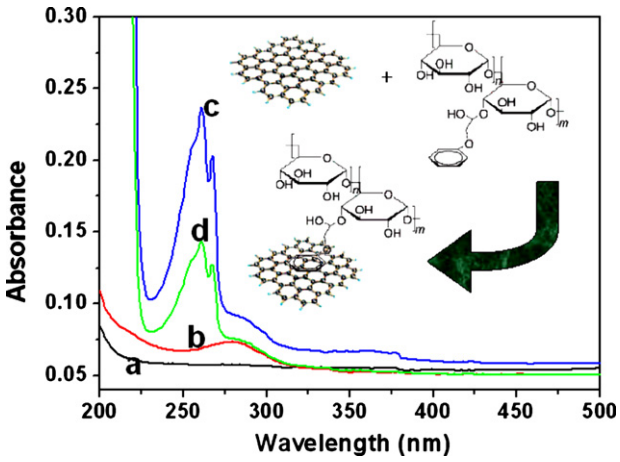

Fig. 1. UV–vis absorption spectroscopy of (a) graphene after interaction with dextran, (b) pure dextran sample, (c) graphene after interaction with DexP, and (d) pure DexP sample.

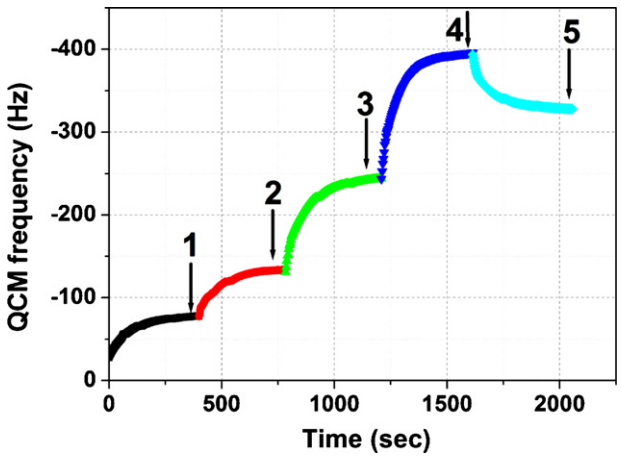

Fig. 2. QCM responses of (arrow 1) bare QCM probe, (arrow 2) graphene on bare QCM probe, (arrow 3) DexP on the GP/Au surface, (arrow 4) ConA on the DexP/GP/Au surface, and (arrow 5) 5 mM glucose on the ConA/DexP/GP/Au surface.

the center piece was the cell body for solution, and the bottom piece was for mounting purpose. The quartz crystal was located between the center and bottom pieces, and the seal was through two O-rings pressed together by four screws. The QCM measurement setup is illustrated in Scheme 1b.

The measurement principle of the QCM sensors is based on the change/shift in the frequency (Δf) before and after the reaction according to the Sauerbrey equation [35]: $\Delta f = -2.3 \times 10^{-6} f_0^2 \Delta m/A$, where Δf is the resonant frequency difference (Hz); f_0 is the basic resonant frequency of the crystal (75.8 Hz); Δm is the mass accumulation on the crystal surface (g); A is the Au surface area (1.47 cm^2). The prepared QCM chip was first mounted one side of the detection vessel. Each of the samples to be analyzed was then introduced into the detection vessel after stabilization of resonance frequency (shift less than 1 Hz min^{-1}). The frequency changes in all experiments were referred to the mean value of triplicate measurements. The measurement process of the QCM sensor for glucose is illustrated in Scheme 1a.

3. Results and discussion

3.1. Construction and characteristics of the graphene-based sensing platform

Scheme 1a represents a schematic illustration of the displacement-based QCM biosensor. As the graphene nanosheets on the gold surface with the ability to stably adsorb biomolecules was reported [36], we anticipated that graphene nanosheets could bind phenoxy-derivatized dextran. The assay is based on the displacement mode similar to the competitive-type immunoassay. Since the moleclar weight of ConA is far more than that of glucose, the displaced ConA using the glucose generates a larger frequency change than that of using small glucose molecule, which results in a sensitive response to the target molecule. To verify this issue, pure dextran and phenoxy-derivatized dextran were initially used for modification of graphene nanosheets. The conjugation process was characterized by using UV–vis absorption spectroscopy (Fig. 1). A adsorption peak at 278 nm was observed at pure dextran sample (Fig. 1b). When the pure dextran was interacted with graphene nanosheets, however, the obtained graphene *via* centrifugation did not display the absorption peak of dextran (Fig. 1a). The result indicated that the pure dextran could not be adsorbed onto the graphene surface. On the contrary, an obvious peak was acquired after the phenoxy-derivatized dextran was incubated with graphene nanosheets (Fig. 1c). The peak mainly derived from the immobilized phenoxydextran (Fig. 1d) due to π–π stacking interactions between graphene nanosheets and 1,2-epoxy-3-phenoxypropane. Such interaction could provide a facile pathway for the conjugation of ConA.

3.2. QCM characteristics of the graphene-based sensors

Fig. 2 shows the QCM responses (frequency *vs.* time) of graphene absorption, DexP assembly, and the subsequent ConA reaction in turn on the bare QCM probe. The initial baseline was obtained when the bare QCM probe was exposed to distilled water (arrow 1). Graphene absorption (arrow 2) was remarkably observed as a result of the increase in the QCM frequency, reflecting the kinetic process of graphene adsorbed onto the gold surface. After flushing with distilled water twice to rinse off the excess graphene nanosheets, the subsequent DexP injection (arrow 3) leaded to a typical QCM response, which represented the binding of the biomolecules on the surface. The increase in the QCM frequency could be used to evaluate the amount of the DexP coupled onto the surface. Following that, ConA sample was injected, and a new baseline was created (arrow 4). The significant increase in the frequency is reflective of the change of the sample property within the evanescent field. Subsequently, when the analyte glucose was injected, the frequency was decreased (arrow 5). The reason might be the fact that the ConA molecules were displaced from the DexP molecules due to the competitive-type reaction between glucose and dextran for ConA molecules. On the basis of the QCM results, we might make a conclusion that the ConA molecules were successfully immobilized on the surface of the QCM probe by using DexP and GP as matrices.

3.3. Elucidation of the glucose-concanavalin A-dextran system

Fig. 3 displays the QCM responses of the DexP/GP/Au probe at various conditions. As shown in Fig. 3a, the basic frequency of the DexP/GP/Au probe was about −304.5 Hz in the distilled water. When 5 mM glucose was added in the cell, the frequency was increased (about −309.8 Hz) (Fig. 3b). The shift in the frequency before and after addition of glucose was about 4.3 Hz. Such a small increase in the frequency indicated that the DexP/GP/Au probe could not almost react with glucose in the absence of ConA. In contrast with those of the DexP/GP/Au probe, the basic frequency of the ConA/DexP/GP/Au probe was about −404.2 (Fig. 3c). According to the Sauerbrey equation, the increase in the frequency derived from the mass accumulation on the DexP/GP/Au probe due to the conjugation of ConA micromolecules. This observation

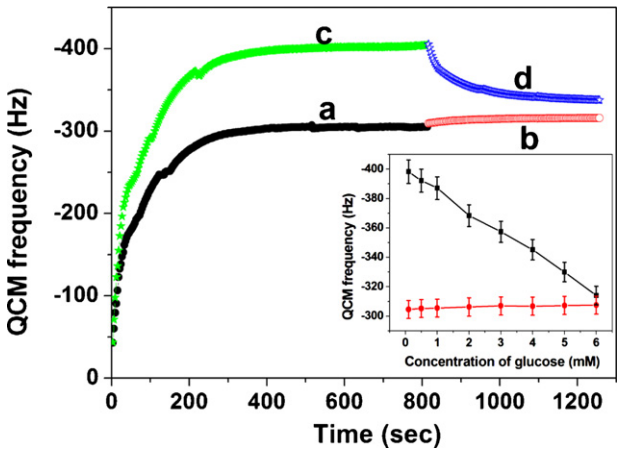

Fig. 3. QCM responses of (a) the DexP/GP/Au, (b) the DexP/GP/Au toward 5 mM glucose, (c) the ConA/DexP/GP/Au, and (d) the ConA/DexP/GP/Au toward 5 mM glucose. *Inset*: Frequency response plots of (●) the DexP/GP/Au and (■) the ConA/DexP/GP/Au toward various glucose standards.

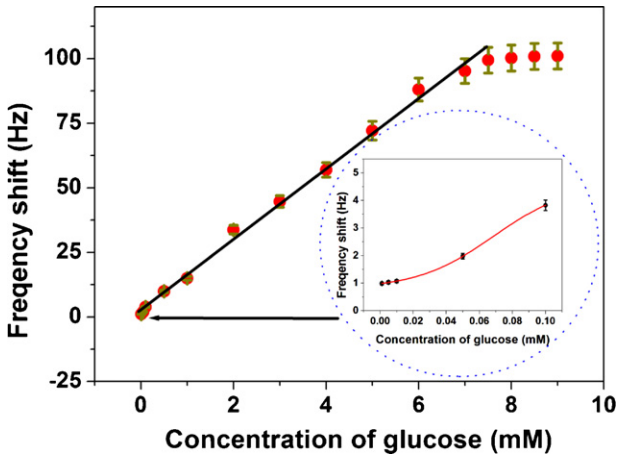

Fig. 5. Calibration curve of the displacement-based QCM sensor for glucose detection. *Inset*: the calibration plots of the QCM sensor at low concentrations of glucose (*Note*: the frequency shift (Δf, Hz) was defined as the absolute value of the frequency difference (Δf).).

indicated the strong interaction between ConA and DexP. Upon addition of 5 mM glucose in the detection cell, the frequency was decreased (about −337.4 Hz) (Fig. 3d), and the shift in the frequency was about 66.8 Hz. The reason for the decrease was due to the displacement of ConA from the surface of the ConA/DexP/GP/Au probe. The inset of Fig. 3 illustrates the QCM responses of the ConA/DexP/GP/Au and DexP/GP/Au probes toward various concentrations of glucose, respectively. In the case of the DexP/GP/Au probe only, no significant variation in the frequency was found in the target concentration range. However, for the ConA/DexP/GP/Au probe, a dramatic decrease in the frequency was observed. These results indicated that the prepared QCM sensors could be used for detection of glucose *via* the displacement-based protocol.

3.4. DexP molecular assembly on the graphene-based surface

For the successful development of QCM sensors, the signal usually depends on the immobilized amount of ligand on the sensor surface. So, the immobilized amount of DexP molecules on the graphene-based surface should be optimised. As shown in Fig. 4a, the conjugated amount of DexP molecules increased with the increment of DexP concentration and leveled off after the concentration of DexP reached 5.0 μM, indicating that DexP has been saturated on the graphene-based surface.

To further monitor the effect of the immobilized amount of DexP molecules on the conjugation of ConA molecules, the as-prepared GP/Au probes modified with various concentrations of DexP were used for the conjugation of ConA. As indicated in Fig. 4b, a largest QCM frequency was observed at 3.0 μM DexP. The phenomenon might be explained by the fact that the quantitative and kinetic differences for the adsorption/immobilization of proteins could be affected by steric hindrance and available reaction sites. Usually, the ratio of DexP in solution results in the same ratio in the substrate surface. Owing to the steric hindrance, the adsorption and immobilization efficiency of the protein decreases. Consequently, greater adsorption occurred on 3.0 μM DexP than that on the other surfaces, from which it can be inferred that 3.0 μM DexP has the optimum combination of reactive sites and steric hindrance. Although 5.0 μM DexP has more reactive sites than that of 3.0 μM DexP, it has larger steric hindrance, resulting in reduced reactivity. Conversely, while high concentration of DexP has significantly more reactive sites, they have greater steric hindrance. Considering these issues, a 3.0 μM DexP was used for the combination of ConA molecules.

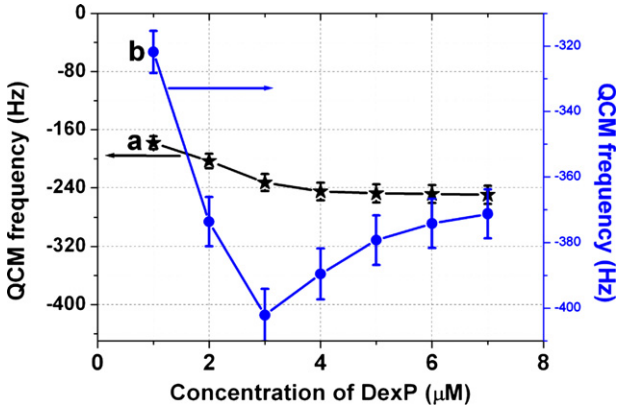

Fig. 4. QCM responses of (a) the GP/Au toward various DexP levels, and (b) the GP/Au modified various concentrations of DexP toward excessive ConA sample.

3.5. Dose–response curve

To monitor the sensitivity and quantitative range of the QCM glucose sensor, a displacement assay mode was employed for detection of glucose by using concanavalin A molecules as traces on the ConA/DexP-functionalized interface. Experimental results indicated that the frequency of the prepared QCM sensor decreased with the increase of glucose concentration. Fig. 5 represents the relationship between frequency shift of the developed QCM sensor and glucose concentration (*Note*: The dose–response curves were calculated on the basis of the frequency shift before and after the interaction with glucose, $\Delta f = f_n - f_0$, where f_n and f_0 are the frequency of the QCM sensor in the presence and absence of glucose, respectively.). As shown in Fig. 5, the frequency shift was proportional to glucose concentration in the range of 0.01–7.5 mM with a detection limit (LOD) of 5 μM at a signal-to-noise ratio of 3σ (where σ is the standard deviation of a blank solution, $n = 13$). The linear regression equation is Δf (Hz) = 7.35 + 31.19 × $C_{[glucose]}$ (mM) ($R^2 = 0.996$). The saturation of dose response in higher concentration of glucose is mainly due to the limitation of ConA binding site. Since the normal level of glucose is 3.3–6.1 mM in human serum, the QCM sensor could completely meet the needs of glucose detection in clinical analysis. When the glucose concentration was higher than 7.5 mM, an appropriate dilution of sample was necessary.

Table 1
Interference degree or crossing recognition level of the displacement-base QCM glucose sensor.

Glucose + interfering agent		$C_{[interfering\ agents]}$ (mM)/frequency shift (Hz)[a]				Mean ± SD (Hz)	RSD (%)
$C_{[glucose]}$ (mM)	Interfering agents	0	0.05	1.0	5.0		
0.05 mM glucose	AA	1.93	2.12	2.24	2.09	2.1 ± 0.11	5.3
	UA	2.04	2.56	2.12	2.17	2.2 ± 0.2	9.0
	BSA	2.16	2.14	1.99	2.14	2.1 ± 0.07	3.2
	AP	1.98	2.28	2.13	2.27	2.2 ± 0.12	5.6
1.0 mM glucose	AA	16.96	19.19	21.15	20.22	19.4 ± 1.6	8.0
	UA	17.12	19.97	19.07	18.34	18.6 ± 1.1	5.6
	BSA	17.09	21.27	19.56	18.21	19.0 ± 1.6	8.2
	AP	17.17	18.12	19.34	20.28	18.7 ± 1.2	6.3
5.0 mM glucose	AA	74.06	77.08	80.46	79.67	77.8 ± 2.5	3.2
	UA	73.91	78.01	77.19	75.16	76.1 ± 1.6	2.1
	BSA	74.18	75.09	77.13	75.27	75.4 ± 1.1	1.4
	AP	73.89	75.98	79.45	76.17	76.4 ± 2.0	2.6

[a] The average value of three successful assays, and the frequency shift was defined as the absolute value of the frequency difference.

Table 2
The recoveries determined using the displacement-based QCM sensor *via* spiking glucose standards into distilled water and blank cattle serum.

Substrates	Spiking value (mM)	Assayed value (Mean ± SD, mM)[a]	Recovery (%)
Distilled water	0.05	0.06 ± 0.01	120
	1.0	0.92 ± 0.27	92
	3.0	3.46 ± 0.98	115.3
	6.0	5.54 ± 1.2	92.3
Blank cattle serum	0.05	0.08 ± 0.02	160
	1.0	1.23 ± 0.35	123
	3.0	3.78 ± 1.78	126
	6.0	6.78 ± 1.12	113

[a] The average of three successful assays.

3.6. Reproducibility and selectivity

The reproducibility of the displacement-based QCM sensor was monitored by assaying 5 glucose levels for 5 replicate measurements in the same run. The relative standard deviations (RSDs) with this method were 4.3%, 3.9%, 6.2%, 4.8% and 5.6% for 0.05, 0.1, 1.0, 3.0, and 6.0 mM glucose, respectively. So, the reproducibility of the QCM sensor is acceptable.

Next, the selectivity of the QCM glucose sensor was also evaluated by using some possible interfering agents, such as L-ascorbic acid (AA), uric acid (UA), bovine serum albumin (BSA) and 4-acetamidophenol (AP). The assay was carried out in 0.05, 1.0 and 5.0 mM glucose solution containing various concentrations of interfering compounds. As shown in Table 1, no obvious difference (RSD ≤ 9.0%) was found in comparison with that of only glucose even if the concentration of interfering compounds was increased. Hence, the selectivity of the QCM-based glucose sensor was acceptable.

3.7. Analysis of real sample

To investigate the applicability of the displacement-based QCM sensor for detection of real samples and the effect of composite matrix on the properties of the QCM sensor, 8 standards with various glucose concentrations were spiked into the distilled water and blank cattle serum using the standard addition method, respectively. (*Notes*: The reason for the use of cattle serum samples is that normal human serum contains certain glucose.) The contents of glucose in these samples were assayed by using the QCM glucose sensor according to the calibration curve. The results are listed in Table 2. As indicated in Table 2, the recoveries were 92–115.3% and 113–160% for distilled water and blank cattle serum, respectively. So, the QCM glucose sensor presented good recovery.

3.8. Comparison with other enzyme and nonenzyme glucose sensors

To embody the advantages of the displacement-based QCM sensor for glucose detection, the analytical properties of the developed sensor were compared with other enzyme and nonenzyme glucose sensors [5,37–47]. The results are summarized in Table 3. Although the dynamic range of the QCM sensor was relatively narrow, the LOD is comparatively low. The reason might be due to the limitation of DexP amount on the QCM crystal. Significantly, the displacement-based QCM sensor not only decreased the cost of the glucose sensor without the need of bioactive enzyme, but also avoided the effects of pH of detection solution and temperature on the sensor performance. Some possible explanations might be attributed to the high sensitivity: (i) Graphene, as a thinnest nanostructure up to date, could favor the fabrication and measurement of QCM sensor; (ii) Concanavalin A is a 26.5-kDa homotetramer with 235 amino acids, and its displacement could generate larger

Table 3
Comparison of analytical properties of the displacement-based QCM glucose sensor with other enzyme and nonenzyme glucose sensors.

Sensor type	Sensor material/or detection method	Dynamic range (mM)	LOD (μM)	Ref.
Enzyme-based glucose sensors	Polyvinylpyrrolidone-protected graphene	2–14	–	[37]
	Polyanimine nanotubes	0.01–5.5	0.1	[38]
	Polyaniline/CNT/SiO_2	1–10	0.1	[39]
	Nano-ZnO	0.01–5.9	10	[40]
	CNT/hydrophobin	05–20	90	[41]
Nonenzyme-based glucose sensors	Nanoporous PtPb networks	1–16	–	[42]
	Polymerized crystalline colloidal array	1–10	–	[43]
	Hollow nano-Pt/porous nano-Au	3.0–7.7	1.0	[44]
	N_2-doped diamond-like carbon electrode with gold nanoclusters	0.25–30	60	[45]
	Co_3O_4 nanofibers	Up to 2.04	0.97	[5]
	Cu_xO/Cu electrode	Up to 4.0	49.0	[46]
	Competitive binding-based FRET	0–30	–	[47]
	Displacement-based mode	0.01–7.5	5.0	This work

frequency shift than that of small molecular glucose; and (iii) Concanavalin A could exhibit higher affinity for glucose than its analogy dextran.

4. Conclusions

In summary, this manuscript describes a sensitive and facile nonenzyme QCM sensor for glucose detection by using a displacement assay format on the graphene-based sensing platform. In the presence of glucose, the immobilized concanavalin A molecules were displaced from the sensor surface through glucose-concanavalin A interaction, resulting in a change in the frequency. Experimental results suggested that the displacement-based QCM glucose sensor could exhibit high sensitivity, good reproducibility and selectivity. Highlight of this study is to replace the detection of small molecules from the determination of macromolecules. Meanwhile, the method also adequately utilized the advantage of graphene for stable adsorption of carbon-based rings. Importantly, the ability to detect such small molecules with low concentrations using the nonenzyme-based displacement mode would find extensively potential applications in unconventional body fluids.

Acknowledgements

We gratefully acknowledge the financial support from the National Science Foundation of China (21075019, 20735002), Research Fund for the Doctoral Program of Higher Education of China (20103514120003), the National "973" Basic Research Program of China (2010CB732403), and the Key Program of Science and Technology Department of Fujian Province (2007Y0026). The authors also sincerely thank the High-Qualified Talent Funding of FZU (XRC-0929) for financial support.

References

[1] P. Martins, M. Haas, S. Obici, Diabetes 59 (2010) 2418–2425.
[2] E. Heyduk, M. Moxley, A. Salvatori, J. Corbett, T. Heyduk, Diabetes 59 (2010) 2360–2365.
[3] L. Zhou, N. Podolsky, Z. Sang, Y. Ding, X. Fan, Q. Tong, B. Levin, R. McCrimmon, Diabetes 59 (2010) 2646–2652.
[4] Diabetes Atlas, 2nd ed., International Diabetes Federation, Bussels, Belgium, 2003.
[5] Y. Ding, Y. Wang, L. Su, M. Bellagamba, H. Zhang, Y. Lei, Biosens. Bioelectron. 26 (2010) 542–548.
[6] G. Ye, X. Wang, Biosens. Bioelectron. 26 (2010) 772–777.
[7] J. Yang, W. Zhang, S. Gunasekaran, Biosens. Bioelectron. 26 (2010) 279–284.
[8] L. Rassaei, F. Marken, Anal. Chem. 82 (2010) 7063–7067.
[9] N. Hashemifard, A. Mohsenifar, B. Ranjbar, A. Allameh, A. Lotfi, B. Etemadikia, Anal. Chim. Acta 675 (2010) 181–184.
[10] M. Arnold, G. Small, Anal. Chem. 77 (2005) 5429–5439.
[11] G. Wilson, R. Gifford, Biosens. Bioelectron. 20 (2005) 2388–2403.
[12] N. Sachedina, J. Pickup, Diabet. Med. 20 (2003) 1012–1015.
[13] R. Wilson, A. Turner, Biosens. Bioelectron. 7 (1992) 165–185.
[14] F. Xiao, F. Zhao, D. Mei, Z. Mo, B. Zeng, Biosens. Bioelectron. 24 (2009) 3481–3486.
[15] X. Kang, Z. Mai, X. Zou, P. Cai, J. Mo, Anal. Chem. 363 (2007) 143–150.
[16] W. Ward, M. Wood, J. Troupe, ASAIO J. 46 (2000) 540–546.
[17] Y. Li, J. Zhang, J. Xuan, L. Jiang, J. Zhu, Electrochem. Commun. 12 (2010) 777–780.
[18] F. Xiao, F. Zhao, Y. Zhang, G. Guo, B. Zeng, J. Phys. Chem. C 113 (2009) 849–855.
[19] S. Sheikh, A. Mulchandani, Biosens. Bioelectron. 16 (2001) 647–652.
[20] http://en.wikipedia.org/wiki/concanavalin_A.
[21] R. Ballerstadt, C. Evans, R. McNichols, A. Gowda, Biosens. Bioelectron. 22 (2006) 275–284.
[22] R. Russell, M. Pishko, C. Gefrides, M. McShane, G. Cote, Anal. Chem. 71 (1999) 3126–3132.
[23] M. Yakovleva, G. Safina, B. Danielsson, Anal. Chim. Acta 668 (2010) 80–85.
[24] Y. Zhao, J. He, M. Yang, G. Gao, G. Zuo, C. Yan, Z. Cheng, Anal. Chim. Acta 654 (2009) 120–126.
[25] R. Say, A. Gultekin, A. Ozcan, A. Denizli, A. Ersoz, Anal. Chim. Acta 640 (2009) 82–86.
[26] X. Jiang, D. Li, X. Xu, Y. Ying, Y. Li, Z. Ye, J. Wang, Biosens. Bioelectron. 23 (2008) 1577–1587.
[27] B. Teo, X. Sun, Chem. Rev. 107 (2007) 1454–1532.
[28] X. Chen, S. Mao, Chem. Rev. 107 (2007) 2891–2959.
[29] K. Yang, B. Xing, Chem. Rev. 110 (2010) 5989–6008.
[30] F. Chen, N. Tao, Acc. Chem. Res. 42 (2009) 429–438.
[31] M. Allen, V. Tung, R. Kaner, Chem. Rev. 110 (2010) 132–145.
[32] C. Lu, H. Yang, C. Zhu, X. Chen, G. Chen, Angew. Chem. Int. Ed. 28 (2009) 4785–4787.
[33] C. Fournier, M. Leonard, I. Lecoqleonard, E. Dellacherie, Langmuir 11 (1995) 2344–2347.
[34] D. Tang, R. Yuan, Y. Chai, Analyst 133 (2008) 933–938.
[35] G. Sauerbrey, Z. Phys. 155 (1959) 2333–2338.
[36] B. Song, D. Li, W. Qi, M. Elstner, C. Fan, H. Fang, Chemphyschem 11 (2010) 585.
[37] C. Shan, H. Yang, J. Song, D. Han, A. Ivaska, L. Niu, Anal. Chem. 81 (2009) 2378–2382.
[38] Z. Wang, S. Liu, P. Wu, C. Cai, Anal. Chem. 81 (2009) 1638–1645.
[39] A. Gopalan, K. Lee, D. Ragupathy, S. Lee, J. Lee, Biomaterials 30 (2009) 5999–6005.
[40] Y. Lei, X. Yan, J. Zhao, X. Liu, Y. Song, N. Luo, Y. Zhang, Colloids Surf. B: Biointerfaces 82 (2011) 168–172.
[41] X. Wang, H. Wang, Y. Huang, Z. Zhao, X. Qin, Y. Wang, Z. Miao, Q. Chen, M. Qiao, Biosens. Bioelectron. 26 (2010) 1104–1108.
[42] J. Wang, D. Thomas, A. Chen, Anal. Chem. 80 (2008) 997–1004.
[43] M. Muscatello, L. Stunja, S. Asher, Anal. Chem. 81 (2009) 4978–4986.
[44] J. Li, R. Yuan, Y. Chai, X. Che, W. Li, X. Zhong, Microchim. Acta (2010), doi:10.1007/s00604-010-0485-z.
[45] A. Liu, E. Liu, G. Yang, N. Khun, W. Ma, Pure Appl. Chem. 82 (2010) 2217–2229.
[46] C. Li, Y. Su, S. Zhang, X. Lv, H. Xia, Y. Wang, Biosens. Bioelectron. 26 (2006) 903–907.
[47] A. Chaudary, M. McShane, R. Srivastave, Analyst 135 (2010) 2620–2628.